Enhanced LPV-based lateral control using ultra-local model-based slip angle estimation

Dániel Fényes, Tamás Hegedűs, Péter Gáspár

***Abstract*— The paper presents a combined observer and lateral control design approach for autonomous vehicles. The goal of the observer design is to estimate the front and rear slip angles of the vehicle together with the cornering stiffness. The observer is based on the combination of the polytopic LPV approach and the ultra-local model. The ultra-local model is used to update the cornering stiffness and, in this way, improve the performance level of the LPV observer. Then, the resulted observer is exploited during the LPV-based lateral control design. The improved lateral control can adapt to different circumstances such as low adhesion coefficient. The proposed observer and LPV controller is implemented and tested in MATLAB/Simulink environment and using the high-fidelity simulation software, CarMaker.**

I. Introduction and motivation

The emergence of highly automated vehicles has many positive effects on society. However, the control design process for highly automated vehicles is challenging due to the nonlinearities, uncertainties, and disturbances present in vehicle dynamics. Therefore, guaranteeing the safe and stable operation of these systems is in the focus of many researchers and companies. Beyond the internal effects, the operation of this system is also influenced by external effects such as the friction coefficient of the given road segment. Therefore guaranteeing the stable motion of vehicles under different road conditions and in various traffic scenarios is a crucial task.

During everyday traffic, the vehicle can encounter an emergency situation, which can only be solved by a trajectory with high lateral acceleration. This implies that the maximum lateral forces, which can be generated by the tires, must be estimated accurately to compute a modified trajectory with which the material damage and injury to people can be avoided. However, in these circumstances, maintaining stable motion is critically important due to the dangerous environment.

D. Fényes, T Hegedűs and P. Gáspár are with Institute for Computer Science and Control (SZTAKI), Hungarian Research Network (HUN-REN), Kende u. 13-17, H-1111 Budapest, Hungary. E-mail: [daniel.fenyes;peter.gaspar]@sztaki.hun-ren.hu

P. Gáspár is with Department for Control of Transportation and Vehicle Systems, Budapest University of Technology and Economics, Stoczek u 2., H-1111 Budapest, Hungary. E-mail: [balazs.nemeth;peter.gaspar]@kjk.bme.hu

The paper was funded by the National Research, Development and Innovation Office under OTKA Grant Agreement No. K 143599. The work of Daniel Fényes was supported by the János Bolyai Research Scholarship of the Hungarian Academy of Sciences.

The research was partially supported by the European Union within the framework of the National Laboratory for Autonomous Systems (RRF-2.3.1-21-2022-00002).

The determination of tire characteristics can be achieved using force and lateral velocity sensors. However, the cost of these sensors is so high that their use in commercial vehicles is not feasible. Moreover, determining tire characteristics after production is also not practical, as these characteristics can change over time. On the other hand, several external effects also influence the characteristics such as the surface of the road or the temperature. This makes it difficult to estimate the tire characteristics in real-time using the onboard sensors of the vehicle.

The estimation process of the tire characteristics can be solved using machine learning-based solutions since these methods can effectively capture the nonlinearities [1]. Although these methods have a high-performance level for the estimation, the degradation and external effects can hardly be involved in the training process. The training performances can be increased by involving the physical information of the vehicle [2]. This method aims to build up a twin model of the car and is suitable mainly for offline tests. The physics-informed neural networks can be used in a control framework such as Model Predictive Control [3], with which motion prediction accuracy can be significantly increased. The results show that the algorithm is capable to control the vehicle accurately, however, the training process of the network still requires a high amount of data. Furthermore, the characteristics can be estimated using the Approximate Bayesian Computation (ABC) method [4], which is also highly depend on the quality and quantity of the data.

On the other hand, classical approaches are also used for the estimation of the tire characteristics. In [5] Particle Swarm Optimization (PSO) and the Unscented Kalman Filter (UKF) methods are used for estimation of the velocity considering velocity-varying tire parameters. Moreover, an estimation method is presented for 6x6 vehicles using the Levenberg-Marquardt algorithm [6]. The main advantage of these methods is that the estimation accuracy is not directly affected by the dataset. Moreover, the estimation within the ranges, which are not covered by the dataset, also provides higher accuracy than a machine learning-based solution. Despite the advantages, the nonlinearities and uncertainties are hard to handle using classical approaches.

In recent years, the ultra-local model-based approach has gained attention. Although the original formalism of the ultra-local model-based structure is developed for control-oriented problems [7], it has potential to use in estimation processes [8]. The method promises that it can take into account the unmodeled dynamics and uncertainintes of the system by the ultra-local model, which is computed from the

input and the derivatives of the output signals.

The paper presents a polytopic LPV-based lateral control solutions, whose performance level is increased by a LPV and ultra-local model-based observer algorithm. The observer estimates the slip angles of the front and rear axles, while the ultra-local model is used to update the cornering stiffness of the vehicle. Then, a lateral control algorithm is proposed, which can utilize the updated cornering stiffness and the estimated slip angles. The operation and the effectiveness of the proposed methods are demonstrated a through a simulation example conducted in MATLAB/Simulink environment and in the CarMaker simulation software.

The structure of the paper is the following: The lateral vehicle dynamics and the modified, slip angle-oriented state space representation of the vehicle is detailed in Section II. The ultra-local model-based approach and the LPV design is briefly described in Section III. The whole observer design can be found in Section III. The lateral control design is presented in Section IV. Finally, a simulation example can be found in Section V, which also includes test scenarios with modified external parameters.

II. Modeling of lateral dynamics

Firstly, the lateral vehicle model is presented in this section. Most of the lateral control-oriented papers use the classical bicycle model, which consists of two state variables: yaw-rate and the lateral velocity or side-slip angle, see [9]. Although this formalism is widely used in lateral control design, it is not suitable for estimating the front and rear slips. Therefore, a modified version is used in this paper, whose states are the slip angles, presented in [10].

A. Modified bicycle model

The original single-track vehicle model has two main equations describing the yaw-motion and the lateral acceleration of the vehicle:

$$I_z\ddot{\psi} = \mathcal{F}_f(\alpha_f)l_f - \mathcal{F}_r(\alpha_r)l_r \tag{1a}$$

$$mv_x(\dot{\psi} + \dot{\beta}) = \mathcal{F}_f(\alpha_f) + \mathcal{F}_r(\alpha_r), \tag{1b}$$

where I_z denotes the yaw-inertia, m is the mass, $\dot{\psi}$ represents the yaw-rate, β is the side-slip of the ceneter of gravity (CoG), v_x is the longitudinal velocity, $\mathcal{F}_i(\alpha_i)\ i \in [f, r]$ is the lateral forces on the front (f) and rear (r) axis as a function of the slips:

$$\alpha_f = \delta - \beta - \frac{\dot{\psi}l_f}{v_x}, \tag{2a}$$

$$\alpha_r = -\beta + \frac{\dot{\psi}l_r}{v_x}, \tag{2b}$$

where δ is the steering angle and l_f, l_r are geometric parameters.

By taking the derivative of the side slips (2) and the equations of the original model (1), the following two equations can be constructed:

$$\dot{\alpha}_r - \dot{\alpha}_f = \frac{l_f + l_r}{I_z}(\mathcal{F}_f(\alpha_f)l_f - \mathcal{F}_r(\alpha_r)l_r) - \dot{\delta} \tag{3a}$$

$$\dot{\alpha}_f l_r + \dot{\alpha}_r l_f = v_x(\alpha_r - \alpha_f) + v_x\delta + l_r\dot{\delta} - \\ - \frac{l_f + l_r}{mv_x}(\mathcal{F}_f(\alpha_f) + \mathcal{F}_r(\alpha_r)) \tag{3b}$$

Using the modified equations (3) a state-space representation can be built up with states of α_f, α_r, more details can be found in [10].

B. State-space representation

The modified bicycle model can be transformed into a parameter-dependent state-space representation. The lateral force function can be linearized in the following way: $\mathcal{F}_i = C_i\alpha_i$. C_i is the cornering stiffness. The cornering stiffness can vary during the operation of the vehicle thus it is handled as a scheduling parameter.

$$\dot{x}_v = A_v(\rho)x_v + B_v(\rho)u_v, \tag{4a}$$

$$y_v = c_v^T(\rho)x_v, \tag{4b}$$

$$\begin{bmatrix}\dot{\alpha}_f \\ \dot{\alpha}_r\end{bmatrix} = \underbrace{\begin{bmatrix}a_{11}(\rho) & a_{12}(\rho) \\ a_{21}(\rho) & a_{22}(\rho)\end{bmatrix}}_{A_v(\rho)}\begin{bmatrix}\alpha_f \\ \alpha_r\end{bmatrix} + \underbrace{\begin{bmatrix}b_1(\rho) \\ b_2(\rho)\end{bmatrix}}_{B_v(\rho)}\delta, \tag{4c}$$

$$ma_y = mv_x(\dot{\beta} + \dot{\psi}) = \begin{bmatrix}C_f(t) & C_r(t)\end{bmatrix}\begin{bmatrix}\alpha_f \\ \alpha_r\end{bmatrix}, \tag{4d}$$

where the output of the system is the lateral force ($m\dot{v}_y = ma_y = mv_x(\dot{\beta} + \dot{\psi})$), and scheduling vector consists of the following variables: $\rho = [C_f(t), C_r(t), v_x(t)]$.
Other parameters of the state-matrices are detailed in [11].

III. Observer design

In this section, the ultra-local model-based observer design is briefly presented for estimating the slip angles of the vehicle. The goal of the ultra-local model is to deal with the parameter uncertainty caused by the cornering stiffness.

A. Ultra-local model

The ultra-local model-based control strategies were presented in [7], [12], [13]. This control technique computes a so-called ultra-local model to deal with uncertainties and unmodelled dynamics. The ultra-local model is continuously update and used as an additional control signal. The ultra-local model is computed from the control signal (u) and the ν^{th} derivative of the output $y^{(\nu)}$:

$$y^{(\nu)} = F + \alpha u, \tag{5}$$

where F is the ultra-local model, α is a tuning parameter, y is the measured output of the system. The ultra-local model can be computed as:

$$F = y^{(\nu)} - \alpha u \tag{6}$$

The ultra-local model is augmented with a traditional controller to guarantee zero steady-state error as:

$$u_{\text{ulm}} = \frac{-F + y_{ref}^{(\nu)} + C(s)e}{\alpha}. \tag{7}$$

The structure of $C(s)$ is not prescribed or restricted it can be freely chosen, such as PID [12] or LQR [14]. The presented ultra-local model will be used in the observer design without any additional controller.

B. LPV-based observer design

The presented polytopic state-space representation has three scheduling parameters, thus an LPV-based observer design is selected, which is briefly detailed in the followings. A general LPV system can be described as, see [15]:

$$\dot{x} = A(\rho)x + B(\rho)u \tag{8a}$$

$$y = c^T(\rho)x + D(\rho)\omega \tag{8b}$$

where: $A(\rho)$, $B(\rho)$, $c^T(\rho)$, $D(\rho)$ are the state matrices, x is the states-vector of the system, u is the control input, y represents the output while ω is the external disturbance.

The goal of the observer design is to minimize the error between the estimated and real states:

$$e = x - \hat{x}, \qquad |e| \to min! \tag{9}$$

where $\hat{x}$ is the estimated state-vector, which can be computed as [16]. The predefined performances can be guaranteed by minimizing the $\mathcal{L}_2$ norm from the disturbances to the performances:

$$\inf_{L(\rho)} \sup_{\rho \in \varrho} \sup_{\substack{\|\omega\|_2 \neq 0, \\ \omega \in \mathcal{L}_2}} \frac{\|z_e\|_2}{\|\omega\|_2}, \tag{10}$$

This optimization problem can be solved by using LMI or Lyapunov function-based solutions, see [17], [18].

C. Combined observer

The structure of the ultra-local model and the LPV-based observer is shown in Figure 1. The LPV observer has three scheduling parameters: cornering stiffness (C_f,C_r) and the longitudinal velocity (v_x). The longitudinal velocity is measurable while the cornering stiffness is computed from the ultra-local model in the following way: The effect of

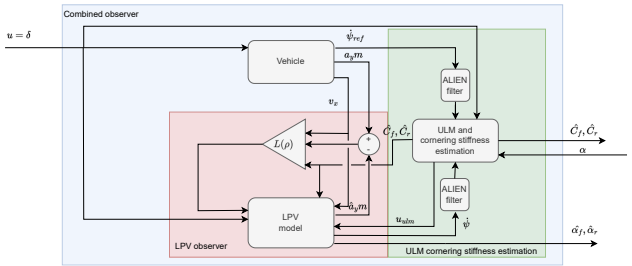

Fig. 1. Schematic structure of the observer

the ultra-local model can be transformed into a deviation of the estimated states ($\Delta\dot{x}_v$). $A_{v,1,1}$ is derived from the state matrix A_v (4) containing that part of the matrix, which is related to the cornering stiffness. The other part of the state matrix A_v is assumed to be constant.

$$\Delta\dot{\hat{x}}_v = A_{v,1,1}(C_{\Delta m}\hat{x}) \tag{11}$$

where $C_{\Delta m} = \begin{bmatrix} \Delta C_f & 0 \\ 0 & \Delta C_r \end{bmatrix}$. Then the change of the cornering stiffness can be computed from the inverted matrix:

$$\begin{bmatrix} -\frac{l_f^2}{I_z v_x} - \frac{1}{m v_x} & \frac{l_f l_r}{I_z v_x} - \frac{1}{m v_x} \\ \frac{l_r l_f}{I_z v_x} - \frac{1}{m v_x} & -\frac{l_r^2}{I_z v_x} - \frac{1}{m v_x} \end{bmatrix}^{-1} \begin{bmatrix} \frac{v_x}{l_f + l_r} + \varphi \\ \frac{v_x}{l_f + l_r} \end{bmatrix} u_{ulm} = \\ = \begin{bmatrix} \Delta C_f \hat{\alpha}_f \\ \Delta C_r \hat{\alpha}_r \end{bmatrix} \tag{12}$$

Finally, the updated cornering stiffness is:

$$\hat{C}_f(t) = \hat{C}_f(t-1) + \Delta C_f(t) \tag{13}$$

$$\hat{C}_r(t) = \hat{C}_r(t-1) + \Delta C_r(t) \tag{14}$$

More details on the observer design can be found in [11].

D. Lateral controller

Since the presented modified bicycle model does not contain the lateral position as a state, it must be augmented in order to guarantee tracking performances. First, the lateral acceleration is computed as:

$$\dot{v}_y = \frac{\alpha_f l_f + \alpha_r l_r}{m} - \left[(\alpha_r - \alpha_f + \delta)\frac{v_x^2}{l_f + l_r}\right] \tag{15}$$

Then, by integrating the lateral velocity, the lateral position can be determined:

$$\dot{x}_e = A_e(\rho)x_e + B_e(\rho)u_e, \quad y_e = c_e^T(\rho)x_e, \tag{16}$$

$$\begin{bmatrix} \dot{\alpha}_f \\ \dot{\alpha}_r \\ \dot{v}_y \\ v_y \end{bmatrix} = \underbrace{\begin{bmatrix} a_{11}(\rho) & a_{12}(\rho) & 0 & 0 \\ a_{21}(\rho) & a_{22}(\rho) & 0 & 0 \\ \frac{l_f}{m} + \frac{v_x^2}{l_f + l_r} & \frac{l_r}{m} - \frac{v_x^2}{l_f + l_r} & 0 & 0 \\ 0 & 0 & 1 & 0 \end{bmatrix}}_{A_e(\rho)} \begin{bmatrix} \alpha_f \\ \alpha_r \\ v_y \\ y_p \end{bmatrix} + \tag{17}$$

$$+ \underbrace{\begin{bmatrix} b_1(\rho) \\ b_2(\rho) \\ -\frac{v_x^2}{l_f + l_r} \\ 0 \end{bmatrix}}_{B_e(\rho)} \delta,$$

IV. LPV CONTROL DESIGN

The main goal of the LPV control design is to guarantee the accurate and stable trajectory tracking of the vehicle even under extraordinary circumstances such as low μ surface. The LPV model has three scheduling parameters: $v_x = \{10-25\} m/s$, $C_f = \{160000-250000\} N/rad$, $C_r = \{160000-250000\} N/rad$. The performances of the control design can be summarized as:

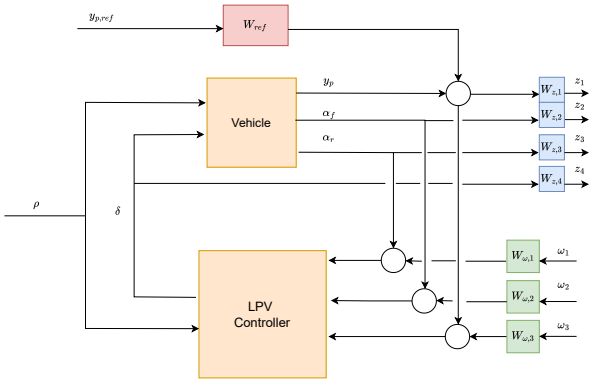

Fig. 2. Augmented plant

- *Trajectory tracking* As the main goal, the controller must guarantee the trajectory tracking of the vehicle, which means the minimization of the error between the reference trajectory (y_{ref}) and the measured position (y).

$$z_1 = y_{p,ref} - y_p, \quad |z_1| \rightarrow min, \tag{18}$$

- *Slip angles* In order ot guarantee the stability of the vehicle, the slip angles of the front and rear axles (α_f, α_r) must be minimized:

$$z_2 = \alpha_f, \quad |z_2| \rightarrow min, \tag{19}$$
$$z_3 = \alpha_r, \quad |z_3| \rightarrow min. \tag{20}$$

- *Intervention* The steering system and the vehicle have their own limitations therefore the intervention also must be minimized:

$$z_4 = \delta, \quad |z_2| \rightarrow min. \tag{21}$$

The presented performances can be achieved by using different weighting functions as shown in Figure IV. For example, the weighting function W_{ref} is used to scale the reference trajectory. Whilst $W_{z,1}$ guarantees the trajectory tracking depending on the frequency. $W_{z,2}$ and $W_{z,3}$ are to minimize the slip angles, while $W_{z,3}$ weights the intervention. Finally, the weighting functions $W_{w,1}$, $W_{w,2}$ and $W_{w,3}$ are to attenuate the noises on the measured signals.

The augmented state-space representation can be written as:

$$\dot{x}_e = A_e(\rho)x_e + B_e(\rho)u_e + B_{e,w}(\rho)w_e, \tag{22a}$$
$$z_e = C_{e,1}(\rho)x_e + D_e(\rho)u_e. \tag{22b}$$

The design of an LPV controller leads to a quadratic optimization problem, which can be solved by selecting an adequate controller ($K(\rho)$). This controller must guarantee the quadratic stability of the closed-loop system. Moreover, the induced $\mathcal{L}_2$ norm from the disturbances to the performances must be smaller than a given value γ.

$$\inf_{K(\rho)} \sup_{\rho \in F_\rho} \sup_{\|w\|_2 \neq 0, w \in \mathcal{L}_2} \frac{\|z\|_2}{\|w\|_2}, \tag{23}$$

where F_ρ bounds the scheduling variables.

V. Simulation Example

In this section, a comprehensive simulation example is presented to show the operation and the effectiveness of the proposed observer and control algorithms. The observer and the controller have been implemented in MATLAB/Simulink environment, while the vehicle model is given by the high-fidelity simulation software, CarMaker. A Tesla Model S has been chosen as the test vehicle. During the simulation the vehicle is driven along a section of the Formula 1 track Suzuka and the adhesion coefficient is set to $\mu = 0.5$.

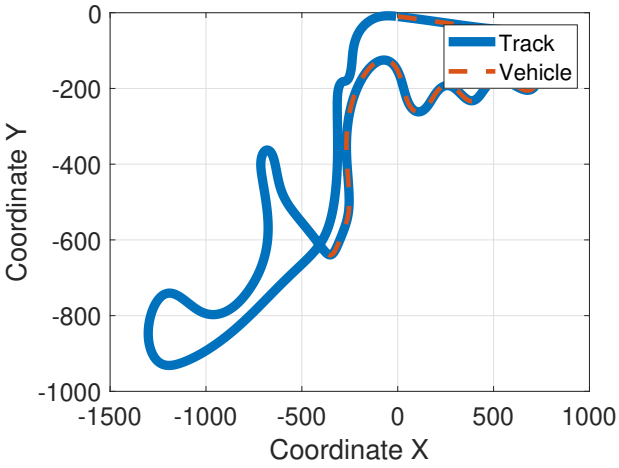

Fig. 3. Test track

The track and the path of the vehicle are shown in Figure 3. The track includes several sharp bends. The vehicle is able to follow the predefined path with high accuracy. The maximal lateral error is around $1m$, which is an acceptable value considering the low adhesion coefficient and the sharp bends.

The longitudinal velocity profile is illustrated in Figure 4, which changes between $v_x \in \{13, 19\} m/s$. The yaw-rate of the vehicle is demonstrated in Figure 5. Its maximal value is around $0.3 rad/s$, which means that the vehicle is close to its psychical on a low adhesion coefficient surface. The lateral acceleration is depicted in Figure 6. Similarly to the yaw-rate, the lateral acceleration also indicates that the vehicle is close to its physical limits since its maximal value is around $0.5 m/s^2$.

The estimation of the front slip angle is shown in Figure 7. The blue line represents the measure value from the CarMaker simulation software, while the red one illustrates the estimated signal. As the result shows, the observer is able to estimate the slip angle with high accuracy, the averaged error is smaller than $< .001 rad$.

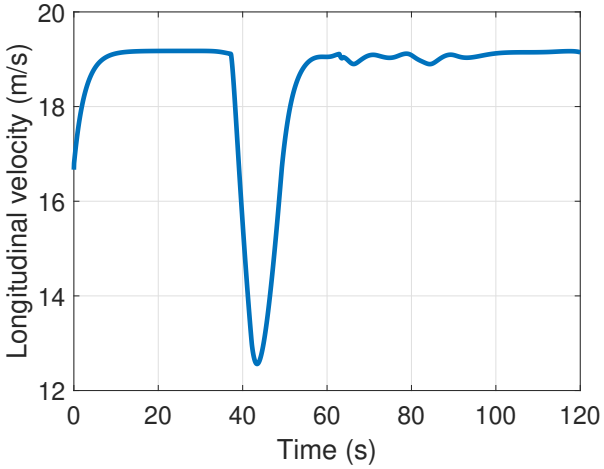

Fig. 4. Longitudinal velocity

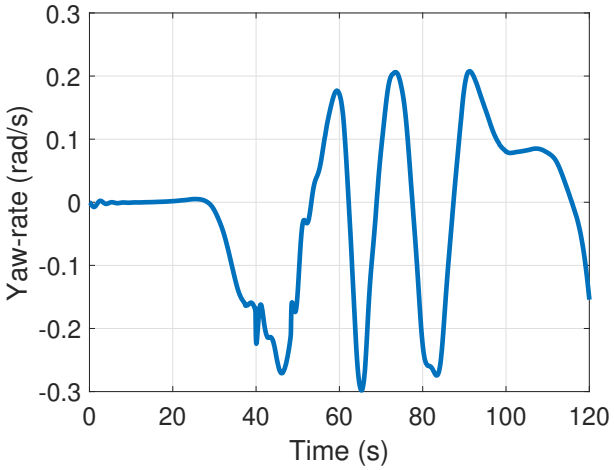

Fig. 5. Yaw-rate

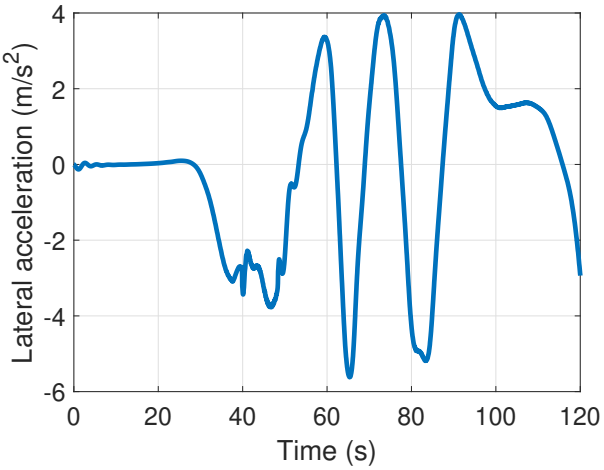

Fig. 6. Lateral acceleration

The cornering stiffness, which is a scheduling parameter of the controller is shown in Figure 8. The output of

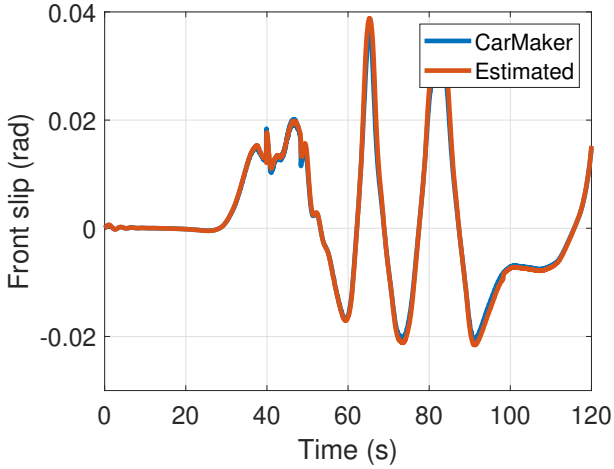

Fig. 7. Front slip angle

the CarMaker is given by the blue line, while the result of the observer is illustrated by the red line. During the simulation, the reference cornering stiffness is computed by the lateral force and the side slip angle ($C = F_y/\alpha$). As the result shows the ultra-local model-based observer is able to estimate the cornering stiffness with high accuracy.

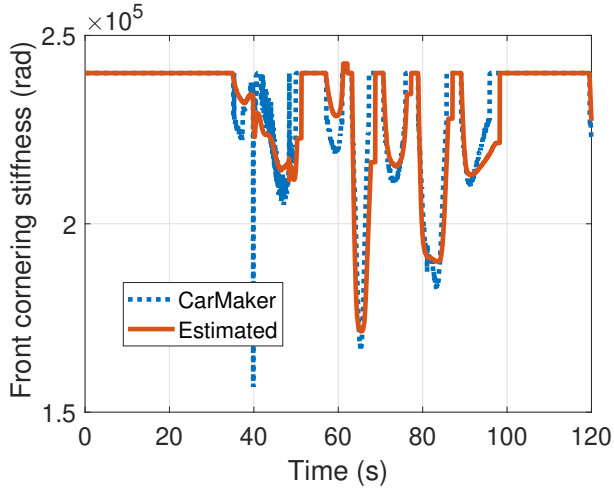

Fig. 8. Front cornering stiffness

Finally, the steering angle is demonstrated in Figure 9. It varies between $\delta \in \{-0.06, 0.04\} rad$, which is a reasonable range for these conditions.

VI. Conclusion

In the paper, a novel slip estimation and lateral control algorithm have been proposed for autonomous vehicles. The slip estimation algorithm was based on the ultra-local model and the polytopic LPV framework, while for the control design, an LPV approach was used. The results of the observer are used as a scheduling variable within the control algorithm. The presented algorithm has been implemented in MATLAB/Simulink connected to the vehicle dynamics simulation software, CarMaker. The methods have been tested

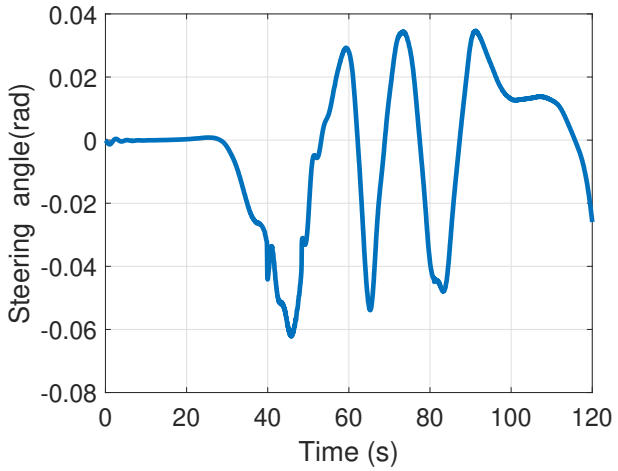

Fig. 9. Steering angle

through a comprehensive simulation example to show their operation and their effectiveness. The presented simulation showed the vehicle was able to follow the predefined path even under extreme circumstances such as a low adhesion coefficient.

REFERENCES

[1] J. L. Olazagoitia, J. A. Perez, and F. Badea, "Identification of tire model parameters with artificial neural networks," *Applied Sciences*, vol. 10, no. 24, 2020. [Online]. Available: https://www.mdpi.com/2076-3417/10/24/9110

[2] T. Hegedus, B. Nemeth, and P. Gaspar, "Identification of tire characteristics using physics-informed neural network for road vehicles," in *2024 32nd Mediterranean Conference on Control and Automation (MED)*, 2024, pp. 706–711.

[3] L. Jin, L. Liu, X. Wang, M. S. Shang, and F.-Y. Wang, "Physical-informed neural network for mpc-based trajectory tracking of vehicles with noise considered," *IEEE Transactions on Intelligent Vehicles*, vol. PP, pp. 1–10, 03 2024.

[4] A. Boyali, S. Thompson, and D. R. Wong, "Identification of vehicle dynamics parameters using simulation-based inference," 2021.

[5] X. Lin, J. Wang, Q. Xu, G. Shi, and Y. Jin, "Real-time estimation of tire-road friction coefficient based on unscented kalman filtering," in *2020 IEEE 5th International Conference on Intelligent Transportation Engineering (ICITE)*, 2020, pp. 376–382.

[6] R. T. d. C. N. Camila Le?o Pereira and B. R. Loiola, "Cornering stiffness estimation using levenberg?marquardt approach," *Inverse Problems in Science and Engineering*, vol. 29, no. 12, pp. 2207–2238, 2021.

[7] M. Fliess and C. Join, "Model-free control," *International Journal of Control*, vol. 86, no. 12, pp. 2228–2252, Dec 2013.

[8] Y. Al Younes, H. Noura, M. Muflehi, A. Rabhi, and A. El Hajjaji, "Model-free observer for state estimation applied to a quadrotor," in *2015 International Conference on Unmanned Aircraft Systems (ICUAS)*, 2015, pp. 1378–1384.

[9] J. Hahn, R. Rajamani, S. You, and K. Lee, "Real-time identification of road-bank angle using differential GPS," *IEEE Transactions on Control Systems Technology*, vol. 12, pp. 589–599, 2004.

[10] T. P. Balazs Nemeth, Peter Gaspar, "Nonlinear analysis of vehicle control actuations based on controlled invariant sets," *International Journal of Applied Mathematics and Computer Science*, vol. 26, no. 1, pp. 31–43, 2016. [Online]. Available: http://eudml.org/doc/276550

[11] D. Fenyes, T. Hegedus, and P. Gaspar, "Estimation of cornering stiffness using ultra-local model and lpv-based observer," in *12th IFAC Symposium on Fault Detection, Supervision and Safety for Technical Processes, SAFEPROCESS 2024*, vol. 58, no. 4, 2024, pp. 437–442.

[12] M. Fliess and C. Join, "Model-free control and intelligent PID controllers: Towards a possible trivialization of nonlinear control?" *Proc. 15th IFAC Symposium on System Identification, Saint-Malo, France*, vol. 42, pp. 1531–1550, 2009.

[13] B. d'Andrea Novel, M. Fliess, C. Join, H. Mounier, and B. Steux, "A mathematical explanation via 'intelligent' PID controllers of the strange ubiquity of pids," *Proc. 18th Mediterranean Conference on Control and Automation*, pp. 395–400, 2010.

[14] Y. A. Younes, A. Drak, H. Noura, A. Rabhi, and A. El Hajjaji, "Robust Model-Free Control Applied to a Quadrotor UAV," *Journal of Intelligent and Robotic Systems*, vol. 84, pp. 37 – 52, Dec. 2016.

[15] R. Toth, *Modeling and Identification of Linear Parameter-Varying Systems*, ser. Lecture Notes in Control and Information Sciences. Berlin, Heidelberg: Springer, 2010, vol. 403.

[16] C. M. Kang and W. Kim, "Linear parameter varying observer for lane estimation using cylinder domain in vehicles," *IEEE Transactions on Intelligent Transportation Systems*, pp. 1–10, 2020.

[17] A. Zemouche, M. Zerrougui, B. Boulkroune, R. Rajamani, and M. Zasadzinski, "A new lmi observer-based controller design method for discrete-time lpv systems with uncertain parameters," pp. 2802–2807, 2016.

[18] C. Briat, O. Sename, and J.-F. Lafay, "Design of lpv observers for lpv time-delay systems: an algebraic approach," *International Journal of Control*, vol. 84, no. 9, pp. 1533–1542, 2011. [Online]. Available: https://doi.org/10.1080/00207179.2011.611950